ISSN 0915-633X

NATIONAL INSTITUTE FOR FUSION SCIENCE

Magnetohydrodynamic Approach to the Feedback Instability

T. -H. Watanabe and T. Sato

(Received - May 13, 1997)

NIFS-495 July 1997

RESEARCH REPORT
NIFS Series

NAGOYA, JAPAN

Magnetohydrodynamic approach to the feedback instability

T.-H.Watanabe and T.Sato
Theory and Computer Simulation Center
National Institute for Fusion Science
322-6, Oroshi-cho, Toki, Gifu 509-52, Japan

Abstract

Starting from the ideal magnetohydrodynamic and two-fluid equations, the linear analysis of the feedback instability has been made in a coupled system of perfectly and partially ionized plasmas. The obtained eigenfunction and frequency of the unstable mode are qualitatively consistent with observations of auroral arcs.

Keywords: magnetohydrodynamics, weakly ionized plasma, auroras

I Introduction

It has been believed that auroral arcs are excited by the magnetosphere-ionosphere (M-I) interaction through the Alfvén wave carrying the field-aligned current. An analogy of an electric circuit was helpful and, thus, frequently employed to understand the local M-I coupling associated with auroral arcs as well as the global one[1−4]. Being based on the idea that a plasma response in the magnetosphere is represented by the impedance of a transmission line, Sato has proposed a theory of auroral arc formation[4]. In his theory, the magnetosphere is treated as a passive media filled with a perfectly ionized plasma, while the ionosphere is considered as an active boundary made of a partially ionized gas.

After the theory succeeded in explaining several important features of auroral arcs, a two-dimensional computer simulation with the transmission line equation has been performed to study global characteristics in appearance of auroral arcs[5]. The assumption of the transmission line has been removed by usage of the magnetohydrodynamic (MHD) equations in a three-dimensional simulation[6]. Using the three-dimensional model of the M-I coupled system, a comprehensive simulation study has been made in a few years ago, where an effect of the parallel electric field has also been considered[7]. A local model of auroral growth coupled with the 'cavity' mode of the Alfvén wave has also been investigated using the MHD equations. Nevertheless, no detailed linear analysis of the feedback instability based on the MHD equations has been presented as of today.

In this paper, starting from the basic equations, we have obtained the linear dispersion relation and eigenfunction in a coupled system of perfectly and partially ionized plasmas. We will also derive the characteristic impedance of the perfectly ionized plasma in the magnetosphere, while it was given by a physical insight into the Alfvén wave in the previous works[3,4,7]. Our MHD approach starting from the basic equations has more generality than the transmission line theory and will give a full understanding to a mechanism of the feedback instability.

II Dispersion relation and eigenfunction

We set x and z coordinates in horizontal and vertical directions. Physical quantities are assumed to have a sinusoidal perturbation in x but an eigenfunction in z, such that, $f(x,z,t) = f(z)\exp(ik_\perp x - i\omega t)$. The system is symmetric in y direction. A linearized set of the ideal MHD equations is given as follows.

$$\frac{\partial B_y}{\partial t} = -\frac{\partial E_x}{\partial z} \ , \tag{1}$$

$$\rho_0 \frac{\partial V_y}{\partial t} = -j_x B_{z0} \ , \tag{2}$$

$$\mu_0 j_x = -\frac{\partial B_y}{\partial z} \quad , \quad \mu_0 j_z = \frac{\partial B_y}{\partial x} \ , \tag{3}$$

and

$$E_x = -V_y B_{z0} \ , \tag{4}$$

where the zero-order magnetic field is parallel to z axis. Notations are conventional. Then, we obtain the following wave equation of the shear Alfvén mode,

$$\frac{\partial^2 E_x(z)}{\partial z^2} = -\frac{\omega^2}{V_A^2} E_x(z) \ . \tag{5}$$

Here, the Aflvén velocity V_A is $B_{z0}/\sqrt{\mu_0 \rho_0}$. Two types of boundary conditions may be imposed on the magnetospheric equatorial plane at $z = \ell$, that is,

$$\text{type I}: \qquad E_x(\ell) = 0 \tag{6}$$

or

$$\text{type II}: \qquad j_z(\ell) = \frac{k_\perp}{\mu_0 \omega} \left. \frac{\partial E_x(z)}{\partial z} \right|_{z=\ell} = 0 \ . \tag{7}$$

Here, the symmetric plasma flow with respect to the equatorial plane is considered in the type II boundary condition, while it is antisymmetric in type I. The eigenfunction $E_x(z)$ is, respectively, given by $E_x(z) = E \sin k_\parallel (z - \ell)$ or $E_x(z) = E \cos k_\parallel (z - \ell)$ for the above boundary conditions. Hence, one will find the well-known dispersion relation of the shear Alfvén waves

$$\omega^2 = k_\parallel^2 V_A^2 \ . \tag{8}$$

It should be noted that $k_{\|}$ as well as ω has an imaginary part when the Alfvén wave grows or decays due to the M-I coupling. Thus, the wave amplitude changes exponentially along field lines. Following the previous work[4], here, we take the type II boundary condition. Therefore,

$$E_x(z) = E\cos k_{\|}(z-\ell) \ , \tag{9}$$

and

$$j_z(z) = -\frac{k_\perp}{\mu_0\omega} k_{\|} E \sin k_{\|}(z-\ell) \ . \tag{10}$$

Height-averaged equations of the ionospheric density perturbation n and the current continuity were given by Sato[4] from the two-fluid equations. Linearizing the equations and assuming that the zero-order electric field E_{x0} is in x direction, we find

$$\frac{\partial n}{\partial t} = \frac{j_z}{eh} - 2\alpha n N_0 + D\frac{\partial^2 n}{\partial x^2} \ , \tag{11}$$

$$\frac{\partial j_{Ix}}{\partial x} = -j_z/h \ , \tag{12}$$

and

$$j_{Ix} = eM_p(nE_{x0} + N_0 E_x) \ . \tag{13}$$

Here, h means thickness of the ionosphere; α is a recombination rate of electrons and ions; N_0 denotes the background density of the ionospheric plasma. In Eq.(11), D is the diffusion coefficient due to collisions with neutral particles[2].

From the above equations, one will obtain that

$$E_x = \frac{j_z}{eh}\frac{1}{ik_\perp N_0 M_p}\left(\frac{ik_\perp M_p E_{x0}}{2\alpha N_0 + Dk_\perp^2 - i\omega} + 1\right) \ . \tag{14}$$

Substituting Eqs.(9) and (10) at $z=0$ into (14), we obtain the dispersion relation of the feedback instability.

$$\omega = k_{\|}V_A = \frac{k_\perp M_p E_{x0}}{1 + i\frac{\mu_0 V_A}{R}\cot(k_{\|}\ell)} - i(2\alpha N_0 + Dk_\perp^2) \tag{15}$$

where the ionospheric resistance R is given by $R = 1/ehN_0M_p$. Comparing Eq.(15) with Eq.(13) of Ref.4, one will find the magnetospheric impedance Z, such that $Z =$

$i\mu_0 V_A \cot(k_{\|}\ell)$. It is noteworthy that Z has the same form with the transmission line theory[4], while $k_{\|}$ is a complex variable here. A quantitative investigation of the linear growth rate is presented in the next section.

III Numerical analysis

Four dimensionless parameters characterizing the dispersion relation of Eq.(15) are defined as follows: $\tilde{Z} = \mu_0 V_A/R$, $\tilde{E} = M_p E_{x0}/V_A$, $\tilde{\alpha} = \alpha N_0 \ell/V_A$, and $\tilde{D} = D/V_A\ell$. Here, ω and k are normalized by $\tilde{\omega} = \omega\ell/V_A$ and $\tilde{k} = k\ell$, respectively. Thus, Eq.(15) is reduced to

$$\tilde{\omega} = \tilde{k}_{\|} = \frac{\tilde{k_\perp}\tilde{E}}{1 + i\tilde{Z}\cot\tilde{k}_{\|}} - i(2\tilde{\alpha} + \tilde{D}\tilde{k}_\perp^2) \ . \tag{16}$$

We have solved Eq.(16) numerically for a set of realistic parameters such as $\tilde{Z} = 2.0$, $\tilde{E} = 1 \times 10^{-3}$ and $\tilde{\alpha} = 1.0$, but, $\tilde{D} = 0$. Fig.1 (a) and (b) show real and imaginary parts of $\tilde{\omega}$ for lower seven harmonics. When $Im(\tilde{\omega}) > 0$, the instability grows. As discussed in Ref.4, the ionospheric density n increases where the upward field-aligned current (positive j_z) exists, when the magnetospheric response is inductive. Then, the high conductive region, i.e., high potential region, induces large j_z. This is why the feedback instability grows. The regions with positive n and j_z are considered as auroral arcs, while negative n and j_z would be regarded as 'black auroras'[9].

As shown in Fig.1, for larger $\tilde{k}_\perp$, the ionospheric perturbation couples with higher harmonics of the shear Alfvén mode which have more growth rates. One can see that $Re(\tilde{\omega})$ approaches to $m\pi$ $(m = 1, 2, ...)$ as $\tilde{k}_\perp$ increases. This is because the eigenfunction to large $\tilde{k}_\perp$ could be approximated by the standing wave solution if $Im(\tilde{\omega}) \ll 1$. More importantly, the unstable solutions are found in a large $\tilde{k}_\perp$ region such as $\tilde{k}_\perp > 2 \times 10^3\pi$, while $\tilde{k}_{\|} \sim m\pi$. Under a realistic parameter of $\ell \sim 6 \times 10^4$km, the most unstable wave length of $m = 1$ mode is about 30km, which is consistent with the typical scale length of auroral arcs in the north-south direction, that is, a few tens of kilometers.

In the above results, the higher harmonic modes will generate finer structures with larger growth rates. The perpendicular diffusion effect, however, would stabilize them in reality. To examine the diffusion effect in the M-I coupled system we have also calculated $\tilde{\omega}$ with a small $\tilde{D}$. The obtained growth rates for $\tilde{D} = 10^{-8}$ are shown in Fig.2. The other parameters are the same as Fig.1. As expected, large $\tilde{k}_\perp$ modes are stabilized by the diffusion effect. The most unstable mode is found at $\tilde{k}_\perp \sim 4 \times 10^3 \pi$ with $m = 2$ under the present parameter. Therefore, the unphysical solution with an infinitely large growth rate in the limit of $\tilde{k}_\perp \to \infty$ can be avoided by introduction of the small $\tilde{D}$. A quantitative estimation of $\tilde{D}$ in the actual ionospheric plasma is necessary for more detailed studies.

IV Concluding remarks

The linear dispersion relation and eigenfunction of the MHD modes are derived from the basic MHD equations in the M-I coupled system with a slab geometry. Numerical solutions of the dispersion relation show a good agreement with the auroral arc observations. Specifically, the characteristic length of auroral arcs in the north-south direction would be explained by the feedback instability that was originally proposed by Sato[4]. The instability analysis presented here, derived from a full MHD description of the magnetospheric plasma, makes further generalization and extension easier. Actually, we are extending our theory to include the compression and/or two-fluid effects, which will be presented elsewhere.

Nonlinear saturation mechanism of the feedback instability is also an important subject remained for future studies. Nonlinearity in the recombination term $(-\alpha n^2)$ and the ionospheric current $(eM_p n E_x)$ would play a key role in the two-dimensional slab geometry considered here, while the $E \times B$ nonlinearity may cause a vortex flow in the three-dimensional case. It is expected that numerical simulations will be helpful to understand a wide variety of nonlinear physics in the coupled system of perfectly and partially ionized plasmas.

References

[1] G.Atkinson, *J.Geophys.Res.*, **74**, 4746, 1970.

[2] T.Ogawa and T.Sato, *Planet.Space Sci.*, **19**, 1393, 1971.

[3] T.Sato and T.E.Holzer, J.Geophys.Res., **78**, 7314, 1973.

[4] T.Sato, J.Geophys.Res., **83**, 1042, 1978.

[5] A.Miura and T.Sato, *J.Geophys.Res.*, **85**, 73, 1980.

[6] K.Watanabe and T.Sato, *Geophys.Res.Lett.*, **15**, 717, 1988.

[7] T.Watanabe, H.Oya, K.Watanabe, and T.Sato, *J.Geophys.Res.*, **98**, 21391, 1993.

[8] R.L.Lysak, *J.Geophys.Res*, **96**, 1553, 1991.

[9] G.T.Murklund, L.G.Blomberg, C.G.Fälthammar, and P.-A.Lindqvist, *Geophys.Res.Lett.*, **21**, 1859, 1994.

Figure captions

FIG.1 Dispersion relation of the Alfvén waves coupled with the ionospheric density change with $\tilde{D} = 0$ for lower seven harmonics: (a) real part of $\tilde{\omega}$ and (b) imaginary part of $\tilde{\omega}$ versus $\tilde{k}_{\perp}$.

FIG.2 Same as Fig.1 but only for $Im(\tilde{\omega})$ with $\tilde{D} = 10^{-8}$.

(a)

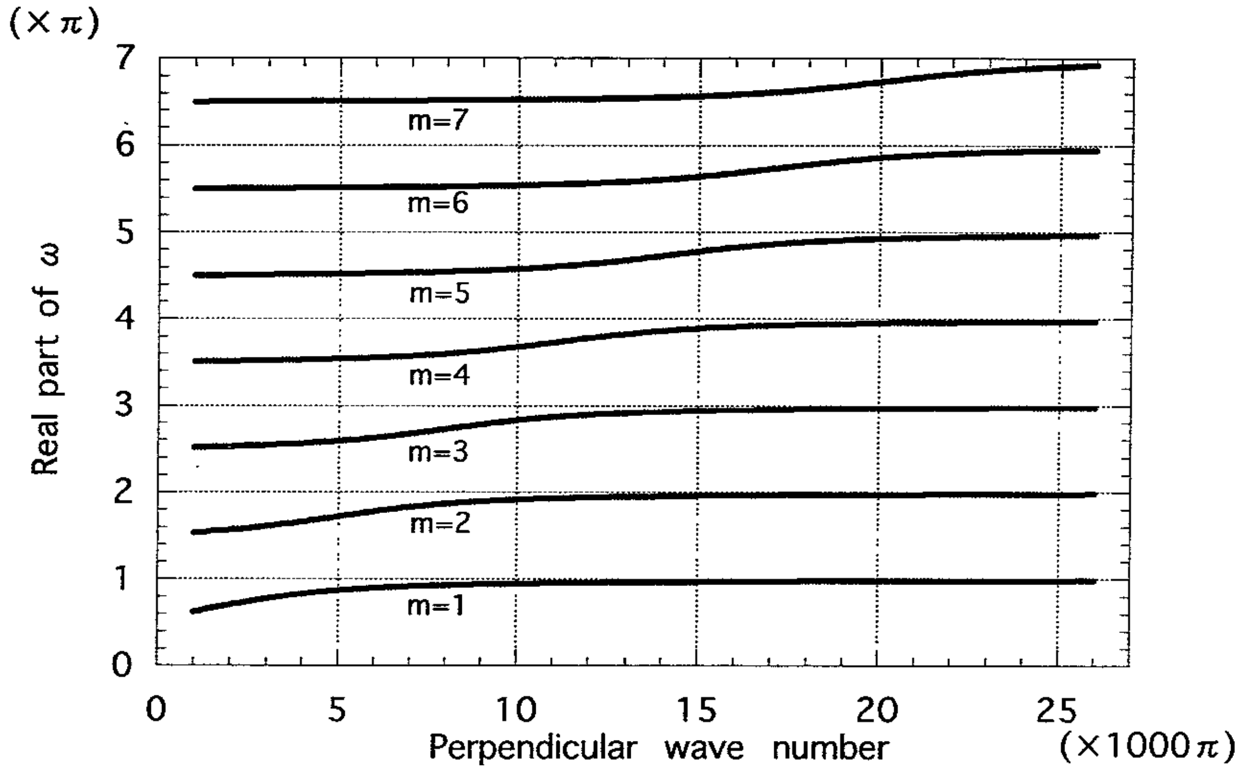
(×π)
7
6
5
4
3
2
1
0
Real part of ω
m=7
m=6
m=5
m=4
m=3
m=2
m=1
0
5
10
15
20
25
Perpendicular wave number
(×1000π)

Fig.1(a)

(b)

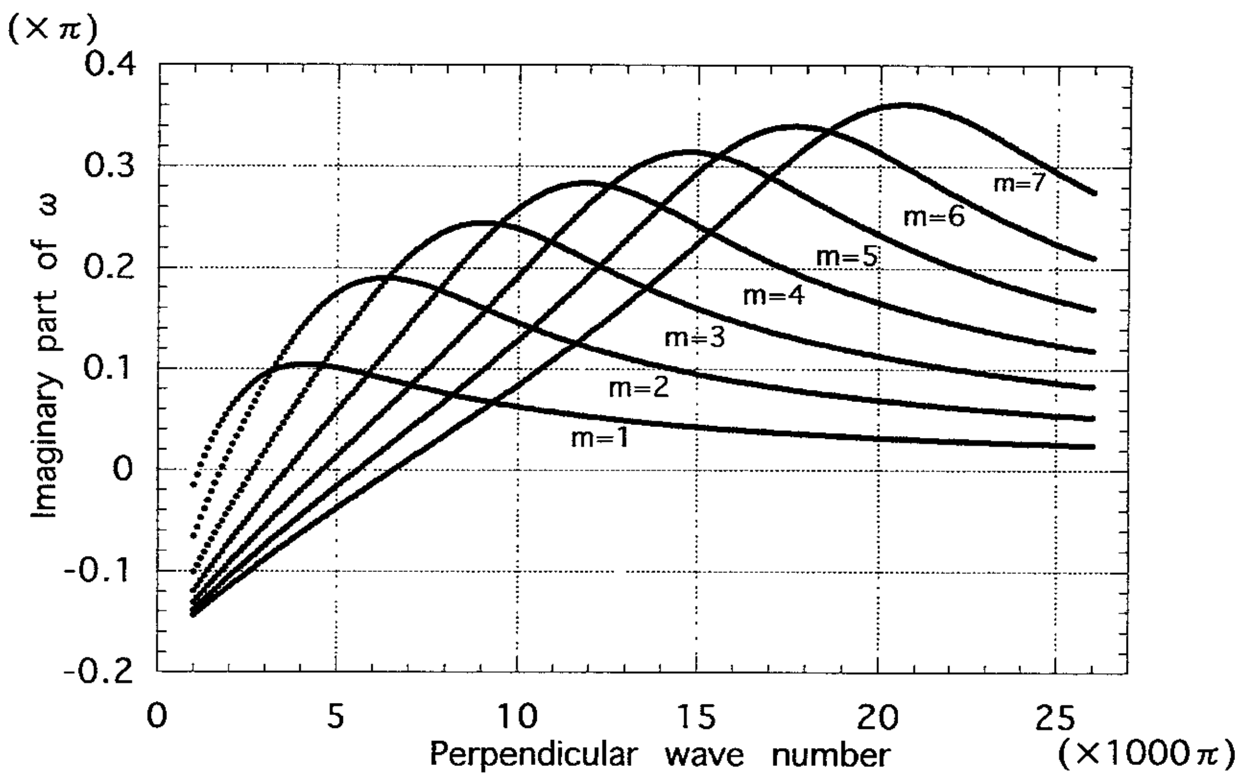
(×π)
0.4
0.3
0.2
0.1
0
-0.1
-0.2
Imaginary part of ω
m=7
m=6
m=5
m=4
m=3
m=2
m=1
0
5
10
15
20
25
Perpendicular wave number
(×1000π)

Fig.1(b)

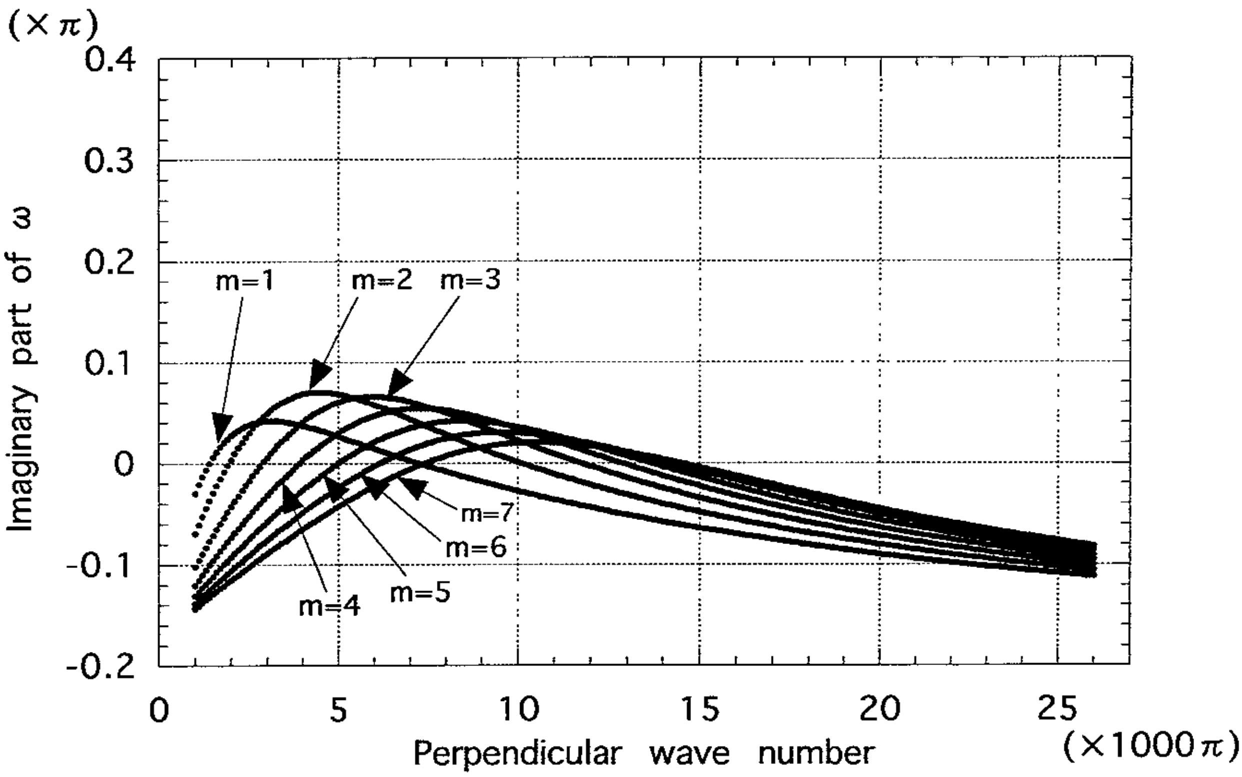
(×π)
0.4
0.3
0.2
0.1
0
-0.1
-0.2
Imaginary part of ω
m=1
m=2
m=3
m=4
m=5
m=6
m=7
0
5
10
15
20
25
Perpendicular wave number
(×1000π)

Fig.2

Recent Issues of NIFS Series

NIFS-449 T. Aoki,
Interpolated Differential Operator (IDO) Scheme for Solving Partial Differential Equations; Sep. 1996

NIFS-450 D. Biskamp and T. Sato,
Partial Reconnection in the Sawtooth Collapse; Sep. 1996

NIFS-451 J. Li, X. Gong, L. Luo, F.X. Yin, N. Noda, B. Wan, W. Xu, X. Gao, F. Yin, J.G. Jiang, Z. Wu., J.Y. Zhao, M. Wu, S. Liu and Y. Han,
Effects of High Z Probe on Plasma Behavior in HT-6M Tokamak; Sep. 1996

NIFS-452 N. Nakajima, K. Ichiguchi, M. Okamoto and R.L. Dewar,
Ballooning Modes in Heliotrons/Torsatrons; Sep. 1996 (IAEA-CN-64/D3-6)

NIFS-453 A. Iiyoshi,
Overview of Helical Systems; Sep. 1996 (IAEA-CN-64/O1-7)

NIFS-454 S. Saito, Y. Nomura, K. Hirose and Y.H. Ichikawa,
Separatrix Reconnection and Periodic Orbit Annihilation in the Harper Map; Oct. 1996

NIFS-455 K. Ichiguchi, N. Nakajima and M. Okamoto,
Topics on MHD Equilibrium and Stability in Heliotron / Torsatron; Oct. 1996

NIFS-456 G. Kawahara, S. Kida, M. Tanaka and S. Yanase,
Wrap, Tilt and Stretch of Vorticity Lines around a Strong Straight Vortex Tube in a Simple Shear Flow; Oct. 1996

NIFS-457 K. Itoh, S.- I. Itoh, A. Fukuyama and M. Yagi,
Turbulent Transport and Structural Transition in Confined Plasmas; Oct. 1996

NIFS-458 A. Kageyama and T. Sato,
Generation Mechanism of a Dipole Field by a Magnetohydrodynamic Dynamo; Oct. 1996

NIFS-459 K. Araki, J. Mizushima and S. Yanase,
The Non-axisymmetric Instability of the Wide-Gap Spherical Couette Flow; Oct. 1996

NIFS-460 Y. Hamada, A. Fujisawa, H. Iguchi, A. Nishizawa and Y. Kawasumi,
A Tandem Parallel Plate Analyzer; Nov. 1996

NIFS-461 Y. Hamada, A. Nishizawa, Y. Kawasumi, A. Fujisawa, K. Narihara, K. Ida, A. Ejiri, S. Ohdachi, K. Kawahata, K. Toi, K. Sato, T. Seki, H. Iguchi, K. Adachi, S. Hidekuma, S.Hirokura, K. Iwasaki, T. Ido, M. Kojima, J. Koong. R. Kumazawa, H. Kuramoto,

T. Minami, I. Nomura, H. Sakakita, M. Sasao, K.N. Sato, T. Tsuzuki, J. Xu, I. Yamada and T. Watari,
Density Fluctuation in JIPP T-IIU Tokamak Plasmas Measured by a Heavy Ion Beam Probe; Nov. 1996

NIFS-462 N. Katsuragawa, H. Hojo and A. Mase,
Simulation Study on Cross Polarization Scattering of Ultrashort-Pulse Electromagnetic Waves; Nov. 1996

NIFS-463 V. Voitsenya, V. Konovalov, O. Motojima, K. Narihara, M. Becker and B. Schunke,
Evaluations of Different Metals for Manufacturing Mirrors of Thomson Scattering System for the LHD Divertor Plasma; Nov. 1996

NIFS-464 M. Pereyaslavets, M. Sato, T. Shimozuma, Y. Takita, H. Idei, S. Kubo, K. Ohkubo and K. Hayashi,
Development and Simulation of RF Components for High Power Millimeter Wave Gyrotrons; Nov. 1996

NIFS-465 V.S. Voitsenya, S. Masuzaki, O. Motojima, N. Noda and N. Ohyabu,
On the Use of CX Atom Analyzer for Study Characteristics of Ion Component in a LHD Divertor Plasma; Dec. 1996

NIFS-466 H. Miura and S. Kida,
Identification of Tubular Vortices in Complex Flows; Dec. 1996

NIFS-467 Y. Takeiri, Y. Oka, M. Osakabe, K. Tsumori, O. Kaneko, T. Takanashi, E. Asano, T. Kawamoto, R. Akiyama and T. Kuroda,
Suppression of Accelerated Electrons in a High-current Large Negative Ion Source; Dec. 1996

NIFS-468 A. Sagara, Y. Hasegawa, K. Tsuzuki, N. Inoue, H. Suzuki, T. Morisaki, N. Noda, O. Motojima, S. Okamura, K. Matsuoka, R. Akiyama, K. Ida, H. Idei, K. Iwasaki, S. Kubo, T. Minami, S. Morita, K. Narihara, T. Ozaki, K. Sato, C. Takahashi, K. Tanaka, K. Toi and I. Yamada,
Real Time Boronization Experiments in CHS and Scaling for LHD; Dec. 1996

NIFS-469 V.L. Vdovin, T.Watari and A. Fukuyama,
3D Maxwell-Vlasov Boundary Value Problem Solution in Stellarator Geometry in Ion Cyclotron Frequency Range (final report); Dec. 1996

NIFS-470 N. Nakajima, M. Yokoyama, M. Okamoto and J. Nührenberg,
Optimization of M=2 Stellarator; Dec. 1996

NIFS-471 A. Fujisawa, H. Iguchi, S. Lee and Y. Hamada,
Effects of Horizontal Injection Angle Displacements on Energy Measurements with Parallel Plate Energy Analyzer; Dec. 1996

NIFS-472 R. Kanno, N. Nakajima, H. Sugama, M. Okamoto and Y. Ogawa,
Effects of Finite-β and Radial Electric Fields on Neoclassical Transport in

the Large Helical Device; Jan. 1997

NIFS-473 S. Murakami, N. Nakajima, U. Gasparino and M. Okamoto,
Simulation Study of Radial Electric Field in CHS and LHD; Jan. 1997

NIFS-474 K. Ohkubo, S. Kubo, H. Idei, M. Sato, T. Shimozuma and Y. Takita,
Coupling of Tilting Gaussian Beam with Hybrid Mode in the Corrugated Waveguide; Jan. 1997

NIFS-475 A. Fujisawa, H. Iguchi, S. Lee and Y. Hamada,
Consideration of Fluctuation in Secondary Beam Intensity of Heavy Ion Beam Prove Measurements; Jan. 1997

NIFS-476 Y. Takeiri, M. Osakabe, Y. Oka, K. Tsumori, O. Kaneko, T. Takanashi, E. Asano, T. Kawamoto, R. Akiyama and T. Kuroda,
Long-pulse Operation of a Cesium-Seeded High-Current Large Negative Ion Source; Jan. 1997

NIFS-477 H. Kuramoto, K. Toi, N. Haraki, K. Sato, J. Xu, A. Ejiri, K. Narihara, T. Seki, S. Ohdachi, K. Adati, R. Akiyama, Y. Hamada, S. Hirokura, K. Kawahata and M. Kojima,
Study of Toroidal Current Penetration during Current Ramp in JIPP T-IIU with Fast Response Zeeman Polarimeter; Jan., 1997

NIFS-478 H. Sugama and W. Horton,
Neoclassical Electron and Ion Transport in Toroidally Rotating Plasmas; Jan. 1997

NIFS-479 V.L. Vdovin and I.V. Kamenskij,
3D Electromagnetic Theory of ICRF Multi Port Multi Loop Antenna; Jan. 1997

NIFS-480 W.X. Wang, M. Okamoto, N. Nakajima, S Murakami and N. Ohyabu,
Cooling Effect of Secondary Electrons in the High Temperature Divertor Operation; Feb. 1997

NIFS-481 K. Itoh, S.-I. Itoh, H. Soltwisch and H.R. Koslowski,
Generation of Toroidal Current Sheet at Sawtooth Crash; Feb. 1997

NIFS-482 K. Ichiguchi,
Collisionality Dependence of Mercier Stability in LHD Equilibria with Bootstrap Currents; Feb. 1997

NIFS-483 S. Fujiwara and T. Sato,
Molecular Dynamics Simulations of Structural Formation of a Single Polymer Chain: Bond-orientational Order and Conformational Defects; Feb. 1997

NIFS-484 T. Ohkawa,
Reduction of Turbulence by Sheared Toroidal Flow on a Flux Surface; Feb. 1997

NIFS-485 K. Narihara, K. Toi, Y. Hamada, K. Yamauchi, K. Adachi, I. Yamada, K. N. Sato, K. Kawahata, A. Nishizawa, S. Ohdachi, K. Sato, T. Seki, T. Watari, J. Xu, A. Ejiri, S. Hirokura, K. Ida, Y. Kawasumi, M. Kojima, H. Sakakita, T. Ido, K. Kitachi, J. Koog and H. Kuramoto,
Observation of Dusts by Laser Scattering Method in theJIPPT-IIU Tokamak
Mar. 1997

NIFS-486 S. Bazdenkov, T. Sato and The Complexity Simulation Group,
Topological Transformations in Isolated Straight Magnetic Flux Tube; Mar. 1997

NIFS-487 M. Okamoto,
Configuration Studies of LHD Plasmas; Mar. 1997

NIFS-488 A. Fujisawa, H. Iguchi, H. Sanuki, K. Itoh, S. Lee, Y. Hamada, S. Kubo, H. Idei, R. Akiyama, K. Tanaka, T. Minami, K. Ida, S. Nishimura, S. Morita, M. Kojima, S. Hidekuma, S.-I. Itoh, C. Takahashi, N. Inoue, H. Suzuki, S. Okamura and K. Matsuoka,
Dynamic Behavior of Potential in the Plasma Core of the CHS Heliotron/Torsatron; Apr. 1997

NIFS-489 T. Ohkawa,
Pfirsch - Schlüter Diffusion with Anisotropic and Nonuniform Superthermal Ion Pressure; Apr. 1997

NIFS-490 S. Ishiguro and The Complexity Simulation Group,
Formation of Wave-front Pattern Accompanied by Current-driven Electrostatic Ion-cyclotron Instabilities; Apr. 1997

NIFS-491 A. Ejiri, K. Shinohara and K. Kawahata,
An Algorithm to Remove Fringe Jumps and its Application to Microwave Reflectometry; Apr. 1997

NIFS-492 K. Ichiguchi, N. Nakajima, M. Okamoto,
Bootstrap Current in the Large Helical Device with Unbalanced Helical Coil Currents; Apr. 1997

NIFS-493 S. Ishiguro, T. Sato, H. Takamaru and The Complexity Simulation Group,
V-shaped dc Potential Structure Caused by Current-driven Electrostatic Ion-cyclotron Instability; May 1997

NIFS-494 K. Nishimura, R. Horiuchi, T. Sato,
Tilt Stabilization by Energetic Ions Crossing Magnetic Separatrix in Field-Reversed Configuration; June 1997

NIFS-495 T. -H. Watanabe and T. Sato,
Magnetohydrodynamic Approach to the Feedback Instability; July 1997